Preparation and Catalytic Performance of the Copper-Manganese-Silicon Catalysts for Dehydrogenation Reaction of 2-butanol

Li Zhang, ChaoQun Chen, XingTong Li and Ying Zhang*
School of Chemical Engineer, Shenyang University of Chemical Technology, Shenyang Liaoning, China.
*syhgxyzhangli@163.com**

(Received on 21st July 2022, accepted in revised form 22 August 2023)

Summary: Cu-Mn-Si catalysts with copper-manganese oxides as the main constituents and silica dioxide as the supports were prepared by co-precipitation method. The performance of the catalysts for the dehydrogenation reaction of the 2-butanol to methyl ethyl ketone was tested. The effects of Cu and Mn ratios on the catalytic performance were investigated. The catalysts were characterized by XRD, SEM, H_2-TPR, TG, BET and XPS, to reveal the catalytic mechanism. The results showed that after adding the manganese, the copper-manganese complexes were formed in the catalysts, which effectively improved the activity of the catalysts. XRD results showed that a new phase of Cu-Mn complex was formed in the fresh catalysts, and reduced copper species appeared in the spent catalysts; TPR results showed that the reduction temperature of the catalysts could be reduced by adding appropriate amount of manganese; XPS results showed that the proportion of Cu^{+}+Cu^0 can be increased in the fresh catalyst and that of Cu^{2+} in the spent catalyst can be decreased after the addition of manganese. When the mole ratio of Cu, Mn and Si in the catalysts was 0.8:0.2:1, the conversion of 2-butanol could reach 94.9%, and the selectivity of methyl ethyl ketone was 98%.

Keywords: Co-precipitation method; Cu-Mn-Si catalyst; Dehydrogenation; 2-butanol; Methyl ethyl ketone.

Introduction

Methyl ethyl ketone can be used as an excellent organic solvent, and as a raw material for fine chemicals for the preparation of fragrances, antioxidants and certain intermediates, and currently extending to fields such as the electronic industry [1]. The main production of methyl ethyl ketone in China and other countries is through the two-step oxidation of n-butene, of which the first step is the reaction of n-butene with water to synthesize 2-butanol. The second step is the dehydrogenation of 2-butanol to methyl ethyl ketone. When the second step of the dehydrogenation reaction is conducted at atmospheric pressure, the selectivity of methyl ethyl ketone is higher and the catalyst life is longer, but the one-way conversion of 2-butanol is lower [2]. On the contrary, when the dehydrogenation reaction is carried out at higher pressure, the catalyst life is relatively short and the selectivity of methyl ethyl ketone is lower. Therefore, the development of catalysts suitable for the dehydrogenation reaction of 2-butanol at atmospheric pressure is very necessary. The traditional catalysts used in the dehydrogenation reaction of 2-butanol are mainly copper-zinc catalysts or zinc oxide catalysts, but the process has the disadvantages of high reaction temperature, large energy consumption and many by-products. At present, more researches have been carried out on copper catalysts. Copper catalysts are focused on copper-zinc-aluminum catalysts and Cu/SiO_2 catalysts. Cu-Zn-Al catalysts has high activity in dehydrogenation reaction. However, due to the strong acidity of Al_2O_3 support, it will promote the side reaction of alcohol hydroxyl dehydration. In this way, the selectivity will be reduced. Cu/SiO_2 catalysts have the advantages of high activity, simple preparation process and no environmental pollution. The catalysts based on Cu/SiO_2 are a hot spot in the study of the dehydrogenation reaction of 2-butanol.

Cu/SiO_2 catalysts are commonly used in hydrogenation and dehydrogenation reactions. March *et al*. [3] investigated the application of Cu/SiO_2 catalysts in the dehydrogenation reaction of isopropanol and found that Cu^0 was the active specie in the catalyst. The deactivation of the catalysts is due to the oxidation of Cu^0. Yang *et al*. [4] prepared a core-shell structure catalyst by the modified Stober method, named as $Cu@mSiO_2$. They sealed Cu nano-particles in mesoporous SiO_2 supports. The conversion of methanol and the selectivity of methyl formate were improved. Li *et al*. [5] prepared Cu/SiO_2 catalysts by the deposition-precipitation method and applied the catalysts for the coupling reactions of dehydrogenation of 2-butanol and hydrogenation of nitrobenzene to aniline. They found that the catalyst rich in Cu (15.9%) has higher specific dehydrogenation rate than that with lower loading (1.8%), because of its larger size of Cu species. Wang *et al*. [6] prepared nano-Cu/SiO_2 catalysts by urea homogeneous precipitation method for the application

*To whom all correspondence should be addressed.

in the hydrogenation reaction of acetophenone. It was found that the catalysts prepared by the urea homogeneous precipitation method had a lower reduction temperature, smaller particle and higher stability. Cu/SiO_2 catalysts also had advantages in activity, selectivity and stability in the hydrogenation reaction of dimethyl oxalate [7].

It has been reported in the literatures that the addition of some reagents to Cu/SiO_2 catalysts could improve their catalytic performance in some reactions. Wu *et al*. [8] added Ca specie to Cu/SiO_2 catalysts by using sol-gel method to catalyze the hydrogenation reaction of furfural. The conversion of furfural and the selectivity of furfural alcohol were improved by increasing the catalyst acidity. Shen *et al*. [9] added Cr specie to Cu/SiO_2 catalysts for the coupling reactions of dehydrogenation of 1,4-butanediol to γ-butyrolactone with hydrogenation of maleic anhydride to γ-butyrolactone. The selectivity of maleic anhydride reached 98%. Tu *et al*. [10] added MgO to Cu/SiO_2 catalysts by the impregnation method. The activity of the catalysts in the dehydrogenation reaction of ethanol was tested. The results showed that the addition of MgO improves the activity and the stability of Cu/SiO_2 catalysts. Deborah *et al*. [11] investigated the catalytic performance of $Cu\text{-}Co/SiO_2$ catalysts for the dehydrogenation reaction of cyclohexanol to cyclohexanone. The results showed that 15%Cu-15%Co/SiO_2 catalysts showed a Cu-Co alloy formation and a higher H_2 chemisorption capacity. Ji *et al*. [12] investigated the catalytic performance of $Cu\text{-}ZnO/SiO_2$ catalysts for the dehydrogenation reaction of cyclohexanol. The results indicated that that the Cu^0 species was the main active site for cyclohexanol dehydrogenation to cyclohexanone and the Cu^+ species was the active site for the aromatization of cyclohexanol to phenol. In addition to these cocatalysts mentioned above, Mn specie was also commonly used as an auxiliary agent to $Cu\text{-}SiO_2$ catalysts to improve their catalytic performance. Fleckensten *et al*. [13] loaded Cu and Mn on SiO_2 supports by using the impregnation method and applied them to the hydrogenation reaction of fatty acid methyl ester. The results showed that the activity, selectivity and stability of catalysts were high. Brands *et al*. [14] applied Cu-Mn-Si catalysts to the hydrogenation reaction of esters and found that the addition of Mn specie to the catalysts improved the dispersity of Cu specie and the activity of the catalysts. Chen *et al*. [15] examined the performance of the Cu-Mn catalysts in the dehydrogenation reaction of methanol, and the study showed that the introduction of Mn specie enhanced the activity and stability of the catalysts. Xu *et al*. [16] studied $Cu\text{-}Mn/In_2O_3$ catalysts in the hydrogenation reaction of ethanol, and a good catalytic performance was achieved due to the improvement of the dispersion of Cu specie. Decyk et al. [17] prepared Cu-Mn-Zn catalysts on different supports and used them in dehydrogenation reaction of isopropyl alcohol. They found that the acidity of Cu-Mn-Zn/dealuminated HY is higher than that of Cu-Mn-Zn/SiO_2. More propylene can be obtained by Cu-Mn-Zn/dealuminated HY while more acetone can be obtained by $Cu\text{-}Mn\text{-}Zn/SiO_2$.

The above literatures shows that Cu-Mn-Si catalyst has not been applied in the dehydrogenation reaction of 2-butanol to methyl ethyl ketone, although it has been used in some dehydrogenation reactions of alcohols. We added Mn specie as an auxiliary agent to Cu/SiO_2 catalysts. The Cu-Mn-Si catalysts were prepared by the co-precipitation method to improve the catalytic performance for the dehydrogenation reaction of 2-butanol by the cooperation effects of Mn and Cu. The catalysts were characterized by BET, H_2-TPR, SEM, XRD, XPS and TG to reveal the catalytic mechanism.

Experimental

Catalysts preparation

The preparation of the catalysts by the co-precipitation method are as follows. The solution of 1mol/L Na_2SiO_3 was slowly added into the mixed solution of 1mol/L $Cu(NO_3)_2$ and 1mol/L $Mn(NO_3)_2$ under the condition of being stirred. The reaction was continued for 2 h at 70 ℃. The precipitate obtained was filtered, washed and dried at 100 ℃~110 ℃ for 24 h, and then calcined at 450 ℃ for 4 h. Finally, the catalyst powder was pressed, crushed and sieved. We obtained the catalyst particles between 20 ~ 40 mesh for the reaction. The catalyst of different mole ratios of Cu to Mn were prepared by adjusting the ratio of $Cu(NO_3)_2$ to $Mn(NO_3)_2$ solutions volume. The nomenclature of the catalyst was marked in mole ratio, such as the catalyst of Cu: Mn: Si=0.8: 0.2: 1, denoted as 0.8Cu-0.2Mn-Si.

Catalyst Characterization

(1) X-Ray Diffractograms (XRD)

The D/max-3C X-ray diffraction instrument was used in the X-ray diffractograms test. The test conditions were as follows. The copper target Ka1 ray was used. The tube current was 150 mA. The tube voltage was 40 KV. The continuous scanning rate was 4 °/min. The scanning step size was 0.02°. The range of the scanning was 15° ~ 80°. The data was collected automatically by a computer.

(2) Scanning Electron Microscope (SEM)

The crystal morphology and crystalline size of the samples were characterized by JSM-6360LV scanning electron microscope. After the samples were processed, photos were taken with the magnification of 2×10^4.

(3) Temperature Programmed Reduction (H_2-TPR)

The amount of the catalysts for the temperature programmed reduction(H_2-TPR) was 50 mg. The test conditions were as follows. The ratio of V(H_2)/V(Ar) was 5: 95. The air flow rate was 45 mL/min ~ 50 mL/min. The heating rate was 10 ℃/min. The temperature was raised from the ambient temperature to 650 ℃.

(4) Thermal Gravimetric (TG)

The thermogravimetric analyzer of Netch TA209 F1 was used in the weight loss experiments in air atmosphere. The test conditions were as follows. The air flow rate was 45 ml/min~50 mL/min. The heating rate was 10 ℃/min. The temperature was raised from the ambient temperature to 900 ℃.

(5) Brunauer Emmett Teller (BET)

The BET surface area (S_{BET}), the total pore volume (V_P) and the mean pore diameter(d_P) were measured after the catalysts were degased at 260 ℃. The N_2 adsorption-desorption curves were measured at -196 ℃. The range of the relative pressure was 0.05~0.30. The specific surface areas (S_{BET}) and the pore volume of the samples were calculated by using the data obtained from the adsorption-desorption experiments.

(6) X-ray Photoelectron Spectroscopic (XPS)

The Axis Ultra multifunctional imaging electron spectrometer of Shimadzu Group of Japan was used in the XPS test. The test conditions were as follows. An aluminum target X-ray source with monochromator was used. The power was about 225 W (operating voltage 15 KV, emission current 15 mA). The energy analyzer was hemispherical.

The evaluation of the catalytic performance

The performances of the catalysts were tested in a continuous fixed-bed reactor. The reactor was made of stainless steel. The length was 260 mm. The inner diameter was 8 mm. The catalysts of 1.0 g (20 ~ 40 mesh) were put into the middle section of the tubular reactor. The upper and the lower sections of the reactor were filled with quartz sands. A thermocouple was placed in the middle section of the packed bed to measure the reaction temperature. Prior to the activity evaluation, the reduction of the catalysts was conducted at 290 ℃, 5%H_2-95%N_2 atmosphere for 2 h. The space velocity of 2-butanol vapor was 5.217 h^{-1}. The dehydrogenation reaction was carried out at 240 ℃, 5%H_2-95%N_2 atmosphere for 4h. The products of the reaction were collected after being condensed. The products were analyzed by GC7890 chromatograph. Chromatographic conditions are as follows. The separation column was PEG-20M capillary column. The detector was FID. The temperature of vaporization chamber was 220 ℃. The shunt ratio was set at 10:1. The temperature of the column was 150 ℃. The area normalization method was used to calculate the fraction of each component.

Results and Discussion

Characterization of the catalysts

XRD

XRD analysis is performed to identify the phases and crystallinity [18]. Fig. 1a shows the XRD patterns of the catalysts with different molar ratios of Cu to Mn. It can be seen from Fig. 1a that the molar ratios of Cu to Mn have significant effects on the structures of the catalysts. The complex oxides of Cu and Mn ($CuMn_2O_4$) and CuO are the main components in Cu-Mn-Si catalysts. There is no obvious diffraction peak of manganese oxides, indicating that Mn species mainly exist in the form of copper-manganese complex oxides. The emergence of the complex oxides means that there was a strong interaction between Cu and Mn species. With the increase of the mole ratios of Cu/Mn, the diffraction peaks of copper-manganese complex oxides become sharper and sharper, which indicates that the crystallinity of the catalysts increases gradually. In Cu-Si catalysts, CuO is the dominant component due to the absence of Mn species. The diffraction peaks are not sharp, which means that CuO species may not exist in a crystalline form or they may highly disperse in the amorphous silica. The diffraction peaks of Mn-Si catalysts are less obvious by the comparison with those of Cu-Mn-Si catalysts. Similar to Cu-Si catalyst, there are no peaks of the copper-manganese complex oxides due to the absence of Cu species. The main component of Mn-Si catalysts may be Mn_2O_3 species which exist in non-crystalline form or they highly disperse in the supports. The crystallite sizes calculated from XRD patterns of the catalysts are shown in Table-1. The crystallite sizes of Cu-Mn-Si catalysts are much larger than those of Cu-Si catalysts and Mn-Si catalysts. This may be due to the formation of the copper-manganese

complex oxides. Among all four kinds of Cu-Mn-Si ternary catalysts, *i.e.*, 0.9Cu-0.1Mn-Si, 0.8Cu-0.2Mn-Si, 0.6Cu-0.4Mn-Si, 0.5Cu-0.5Mn-Si, the catalyst of 0.9Cu-0.1Mn-Si have the highest crystallinity and the smallest crystallite size.

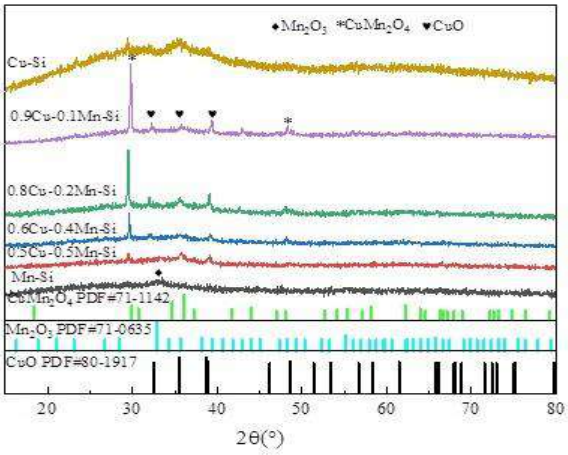

Fig. 1a Fresh catalysts.

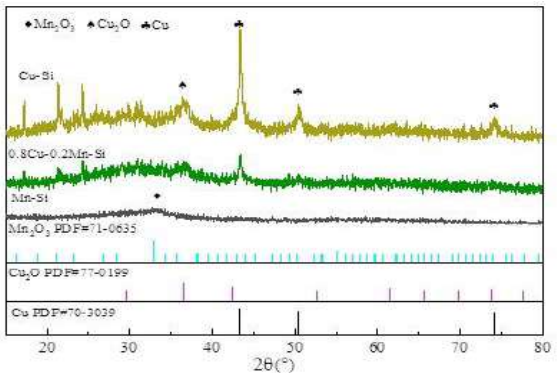

Fig. 1b Spent catalysts.

Fig. 1: XRD patterns of catalysts at different mole ratios.

Table-1: Crystallite size calculated from XRD patterns of the catalysts (The unit is nm.)

Cu-Si	0.9Cu-0.1Mn-Si	0.8Cu-0.2Mn-Si	0.6Cu-0.4Mn-Si	0.5Cu-0.5Mn-Si	Mn-Si
4.41	39.47	43.79	51.51	44.21	12.39

Table-2: Summary of TG results of fresh catalysts.

Sample	Mn-Si	0.5Cu-0.5Mn-Si	0.8Cu-0.2Mn-Si	Cu-Si
TG-step-1(ML%)	6.24	5.51	7.67	0
TG-step-2(ML%)	0	0.81	4.05	4.27
Total (ML%)	6.24	6.32	11.72	4.27

Table-3: Data of specific surface area and pore structure of fresh and spent catalysts.

catalyst	BET specific surface area/(m^2/g)	pore volume/(cm^3/g)	pore diameter/(nm)
Fresh 0.5Cu-0.5Mn-Si	69.23	0.106	15.78
Spent 0.5Cu-0.5Mn-Si	56.47	0.106	20.16
Fresh 0.8Cu-0.2Mn-Si	35.68	0.059	14.64
Spent 0.8Cu-0.2Mn-Si	10.57	0.026	31.83

Fig. 1b shows the XRD patterns of the spent catalysts with different molar ratios of Cu to Mn. It can be seen from Fig. 1b that there are some diffraction peaks of Cu and Cu_2O in spent 0.8Cu-0.2Mn-Si catalysts and Cu-Si catalysts while there are no these diffraction peaks in spent Mn-Si catalysts. There is only a wide peak of Mn_2O_3 in it. Compared with the diffraction peaks of the fresh catalyst in Fig. 1a, it can be seen that the diffraction peaks of Cu-Mn complex at 29.8° and 48° have almost disappeared in the spent catalysts. These results show that the crystal phase in the catalysts has changed significantly through the reduction process. The XRD results showed that more reduced copper species were generated.

It can be seen that the diffraction peaks of Cu and Cu_2O in Cu-Si catalysts are sharper while those of 0.8Cu-0.2Mn-Si catalysts are flatter. This shows that copper species are more dispersed in the latter. This is due to the formation of copper-manganese complex in the process of catalyst preparation. The presence of manganese species improves the dispersion of copper species.

Table-4: Binding energy and contents of copper species in fresh and spent catalysts.

Catalyst	Cu 2p3/2 (eV)		Cu 2p1/2 (eV)		Cu^{2+} /%	$Cu^{+}+Cu^{0}$ /%	$(Cu^0+Cu^+)/Cu^{2+}$
	Cu^{2+}	Cu^0+Cu^+	Cu^{2+}	Cu^0+Cu^+			
Fresh 0.8Cu-0.2Mn-Si	934.75 941.37 943.7	933.81	955.67 962.26	954.4	66.3	33.7	0.508
Spent 0.8Cu-0.2Mn-Si	934.17 942.59 944.31	932.12	954.37 962.53	952.02	46.1	53.9	1.16
Fresh Cu-Si	934.77 941.45 943.66		954.89 962.32		100	0	0
Spent Cu-Si	934.49 941.03 943.50	932.11	954.74 962.36	952.05	48.56	51.44	1.05

SEM

In order to observe the morphology and the size of the catalysts [19], the catalysts were characterized by SEM. Fig. 2 shows the SEM of catalysts with different Cu and Mn mole ratios.

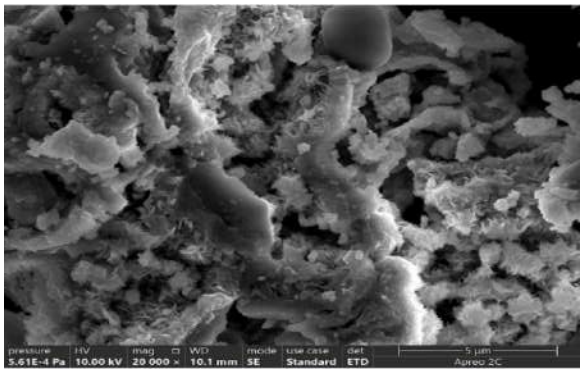

Fig. 2a Cu-Si.

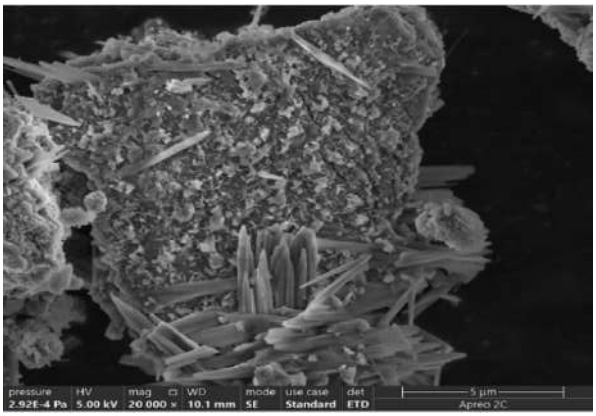

Fig. 2b: 0.9Cu-0.1Mn-Si.

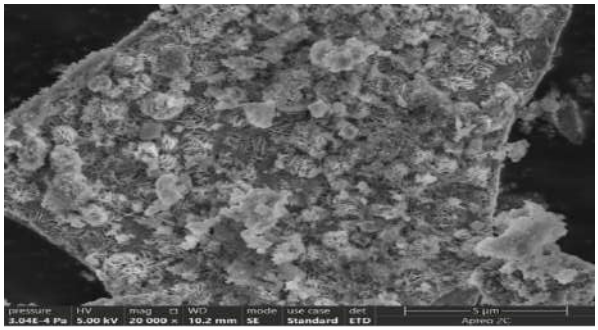

Fig. 2c: 0.8Cu-0.2Mn-Si.

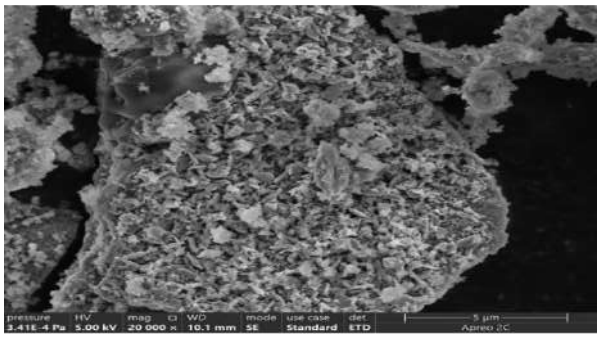

Fig. 2d: 0.6Cu-0.4Mn-Si.

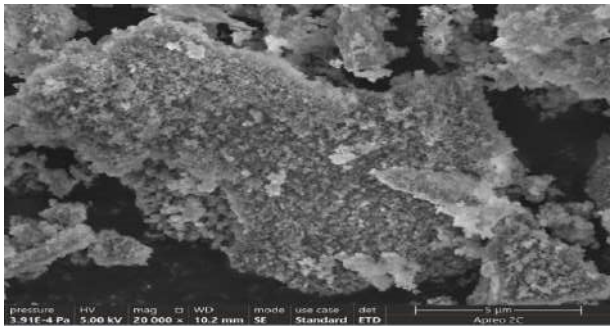

Fig. 2e: 0.5Cu-0.5Mn-Si.

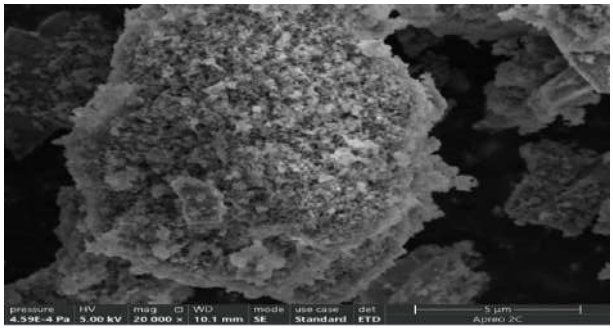

Fig. 2f: Mn-Si.

Fig. 2: The SEM images of catalysts at different mole ratios.

It can be seen from Fig. 2 that the particles of Cu-Si, Mn-Si and 0.5Cu-0.5Mn-Si catalysts are more uniform. In contrast, many large agglomerates are found in 0.6Cu-0.4Mn-Si, 0.8Cu-0.2Mn-Si and 0.9Cu-0.1Mn-Si catalysts. These agglomerates are composed of primary particles. Among all Cu-Mn-Si catalysts, the catalysts of 0.5Cu-0.5Mn-Si have the best dispersion and the most uniform particle size. It is worth noting that in addition to some agglomerates, there are some extra needle-like crystals in 0.8Cu-0.2Mn-Si and 0.9Cu-0.1Mn-Si catalysts. The sizes of the needle-like crystals in catalyst 0.8Cu-0.2Mn-Si are smaller.

H_2-TPR

The reducibility of the catalysts is investigated by H_2-TPR. Fig. 3 shows the H_2-TPR profiles of the catalysts with different molar ratios of Cu to Mn. The lower the reduction temperature, the easier for the catalysts to be reduced. It can be seen from Fig. 3, the Cu-Si catalysts have two reduction peaks at 310 ℃and 520 ℃ respectively. The area of the reduction peak at 520 ℃ was larger, which indicates that the main components of the catalysts are not easy to be reduced. Being referred to Fig. 1, these components may be oxides of copper. When a small amounts of Mn species are added into Cu-Si catalysts to produce 0.9Cu-0.1Mn-Si catalysts, the area of the reduction peak at low temperature (310 ℃) of the catalysts (0.9Cu-0.1Mn-Si) becomes smaller. This should be related to the formation of the Cu-Mn complex. Two new reduction peaks appeared at 470 ℃ and 560 ℃ respectively. These two peaks belong to the reduction of oxides of copper. However, it can be seen that the morphology or structure of copper oxide has changed due to the addition of manganese. The reduction characteristics of 0.9Cu-0.1Mn-Si catalysts are not improved due to the inappropriate mole ratio of Cu to Mn. It can be deduced that this might be related to its high crystallinity by referring to Fig. 2b. For 0.8Cu-0.2Mn-Si, 0.6Cu-0.4Mn-Si, 0.5Cu-0.5Mn-Si catalysts, there was only one reduction peak at lower temperature in the H_2-TPR profiles. The reduction peaks at higher temperature disappeared, which means that the reducibility of the catalysts have been well improved. The 0.8Cu-0.2Mn-Si catalysts has the lowest reduction temperature, indicating that it is the most easily reduced one. The reduction peak of Mn-Si catalysts represents the reduction of Mn_2O_3. The reduction temperature is about 345 ℃.

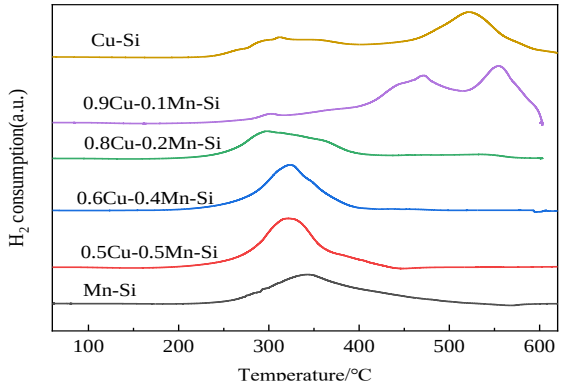

Fig. 3: TPR profiles of Cu-Mn-Si catalysts at different mole ratios.

Being referred with XRD and H_2-TPR, it can be seen that a certain amount of copper-manganese complex oxides could be generated when Mn species are added into Cu/SiO_2 catalysts. If the amount of Mn specie is appropriate, the reduction temperature of the catalysts could be lowered. Accordingly, the reducibility of the catalysts could be improved.

TG analysis

TG analysis is utilized to test the thermal decomposition characteristic of the catalysts [20, 21]. Fig. 4 shows the TG profiles of the fresh catalysts. Table-2 shows the weight loss percentage in the TG process of the fresh catalysts. It can be seen from Fig. 4 and Table-2 that the catalysts had two peaks in the weight loss process after 300 ℃. The weight loss may be caused by the decomposition of different types of oxides of copper and manganese. For the catalysts with different mole ratios of Cu to Mn, the beginning and the ending temperature of the two weight loss peaks are not the same. The amounts of the weight loss are also different. When the manganese contents are higher, the initial decomposition temperatures are lower and the amounts of the weight loss in the secondary decomposition process are less. On the contrary, when the copper contents are higher, the initial decomposition temperature and the amounts of the weight loss in the secondary decomposition process are higher. It is speculated that the weight loss in the first step might be caused by the decomposition of copper - manganese complex oxides and the weight loss in the second step might be caused by the decomposition of oxides of copper. Among them, the Cu-Si catalysts have the highest decomposition temperature and the lowest weight loss. The catalysts of 0.8Cu-0.2Mn-Si have a great weight loss in both the first and the second step. It can be seen from Table-2, the values are 7.674% and 4.053% respectively. The more weight loss of decomposition in the first stage for 0.8Cu-0.2Mn-Si catalysts may be due to the more Cu-Mn complex formed in it.

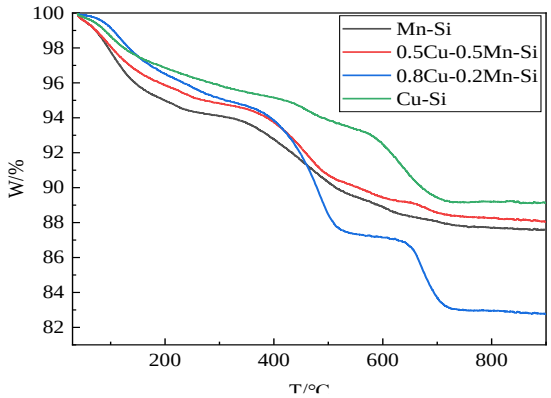

Fig. 4: TG profiles of the fresh catalysts.

Analysis of catalysis and deactivation

Analysis of active sites

Fig. 5 shows TG profiles of the spent catalysts. It can be seen from Fig. 5 that there are a certain amounts of weight loss for all the spent catalysts. It may be caused by the combustion of a certain amount of coke which are deposited on the catalysts surface during the reaction process. After being heated in the air, the deposited carbon could burn out. The weight loss also can be caused by the high-temperature decomposition of the compounds of copper and manganese. However, except for 0.5Cu-0.5Mn-Si catalysts, the weight of other catalysts increases when the temperature is up to 300 ℃. This may be due to the presence of reduced species of copper and manganese, such as Cu^0, Cu^+ and Mn^0, in the spent catalysts. These reduced species (see Fig. 1b) are oxidized during the heating process in the air. Thus, the weight of the catalysts increased. It can be seen from Fig. 4 and Fig. 5 there are obvious differences in the weight loss between the fresh and the spent catalysts. These differences are caused by a combination of the loss due to the burning of the coke and the decomposition of the compounds and the increase due to the oxidation of the reduced species. Among all the catalysts, there are significant weight gains of Cu-Si, Mn-Si and 0.8Cu-0.2Mn-Si catalysts, which indicates that more reduced species of copper and manganese are produced due to the reduction of H_2 during the reaction for those three catalysts. Being compared with Fig. 7, it can be seen that Mn-Si catalyst has the worst catalytic performance although a large amounts of reduced species of manganese are produced in the reaction. Therefore, it could further prove that the reduced species of manganese are not the active sites of the catalysts while the reduced species of copper are the active sites of the catalysts.

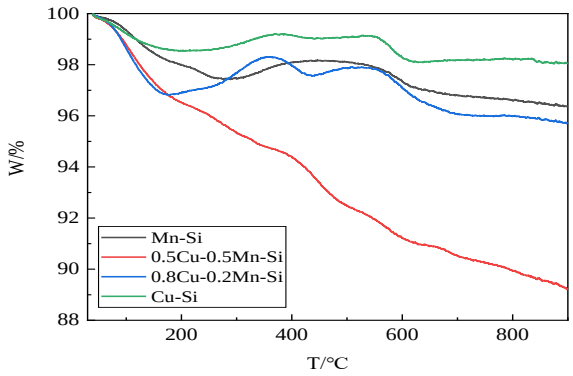

Fig. 5: TG profiles of spent catalysts.

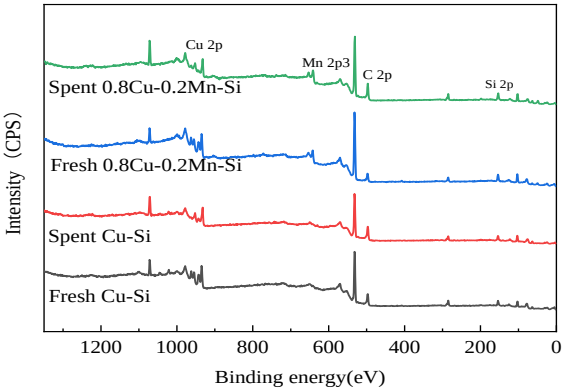

Fig. 6a: Survey.

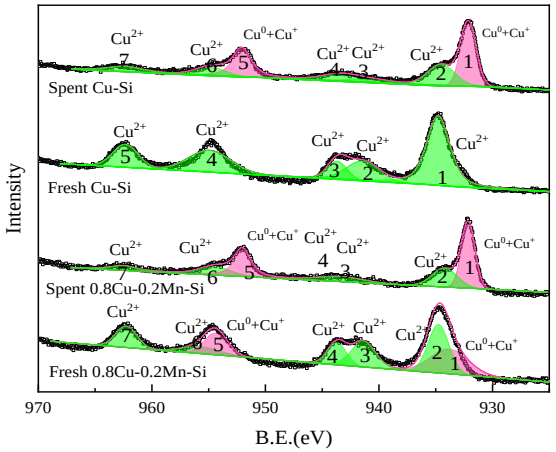

Fig. 6b: Cu 2p scan in Cu-Mn-Si catalysts.

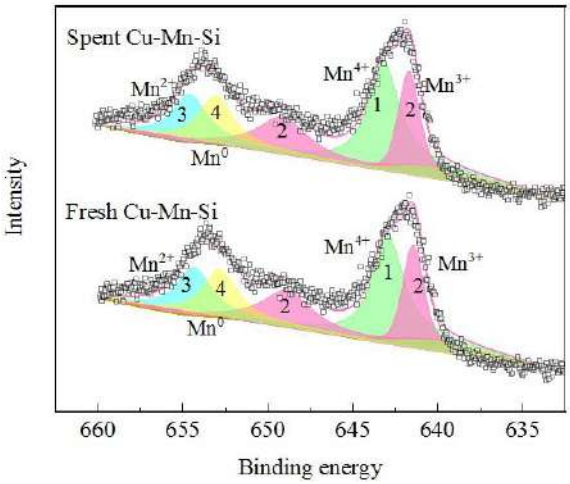

Fig. 6c: Mn 2p scan in Cu-Mn-Si catalysts.

Fig. 6: XPS profiles of fresh and spent catalysts.

For the 0.5Cu-0.5Mn-Si catalysts, there is no weight gain peak. The reason for that may be that the sum of the loss due to the burning of the coke and the decomposition of the copper-manganese compounds is greater than the increase of the oxidation of the reduced species. However, it is unlikely that a large amounts of weight loss of 0.5Cu-0.5Mn-Si catalyst are caused by the burning of its lower activity (see Fig.7). Its more wight loss may be caused by the decomposition of the copper-manganese compounds in the spent catalysts which have not been totally reduced before the reaction. This can be confirmed by Fig. 3. It can be seen from Fig. 3 that 0.5Cu-0.5Mn-Si has poor reducibility compared with Cu-Si, 0.8Cu-0.2Mn-Si, which indicates that under the same conditions, this catalyst generates fewer reducing species. In other words, under the same conditions, this catalyst may require longer reduction time. It can be seen from Fig. 7 that the conversion by using this catalyst has an increasing trend over time, which may be caused by the incomplete reduction of this catalyst before the reaction, while the reduction reaction is still in progress during the reaction process. These TG results also showed the importance of the reducibility of the catalyst to its catalytic performance.

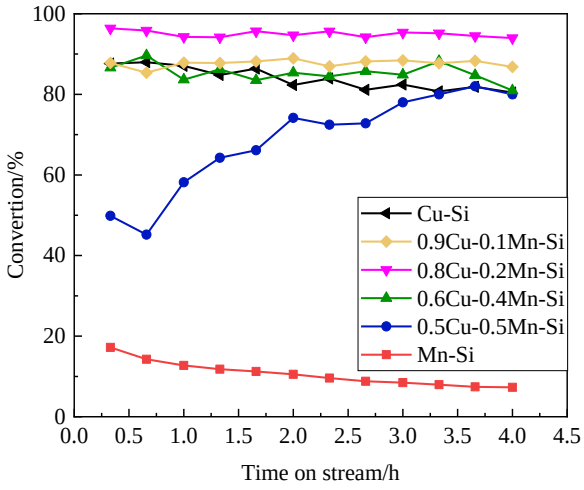

Fig. 7: Influence of Cu/Mn mole ratios on 2-butanol conversion.

Specific surface area and pore analysis

In order to observe the specific surface, pore volume and pore diameter of the catalysts, the catalysts were characterized by BET. Table-3 shows the data of the specific surface area and the pore structure of the fresh and the spent catalysts. It can be seen from Table-3 that the specific surface area, the pore volume and the pore diameter of the fresh catalysts decrease with the increase of the molar ratios of Cu to Mn. It indicates that the catalysts particles accumulate and become larger with the increase of the molar ratios of Cu to Mn. These results are consistent with the results of XRD and SEM (in Fig. 1a and Fig. 2). By comparing with those of the fresh catalysts, the specific surface areas of the spent catalysts become smaller, which may be caused by the deposition of the coke in the reaction. The enlargement of the pore diameter in the spent catalysts may be caused by the reduction of the oxides by H_2 because the discharge channels of steam will be produced in the reduction. By comparing with the data of the fresh and the spent catalysts between 0.5Cu-0.5Mn-Si and 0.8Cu-0.2Mn-Si catalysts in Table-3 and the data in Fig. 7, it can be seen that the catalyst of 0.8Cu-0.2Mn-Si has the higher conversion although it has a smaller initial specific surface area, pore volume and pore diameter. It indicates that compared with other properties, such as composition and reducibility, the specific surface area and the structures of the pores of the catalysts may not be the most important factors to determine the performance of catalysts. From the differences of pore diameter between the fresh and the spent catalysts, it can be seen that the reducibility of the catalysts may be a key factor to determine the performance of catalysts. The larger pore diameter of the catalysts means that more reduced substances, *i.e.*, Cu^0, Cu^+ are generated in the reaction. The reason is that the more formation of Cu^0, Cu^+ will release more steam, which plays a role of pore expansion. From Table-3, it can be seen that there is a significant change of the pore diameter between the fresh and the spent catalysts of 0.8Cu-0.2Mn-Si, which means that more reduced substances are produced in the reaction. These results are consistent with those in Fig. 3 which indicates that 0.8Cu-0.2Mn-Si catalysts are more easily to be reduced than 0.5Cu-0.5Mn-Si.

XPS characterization

The results obtained by TG and BET show that the amount of the reduced copper species in the catalysts may be the main factor to determine the performance of the catalysts. XPS can study the chemical state and composition of elements on catalyst surface [22, 23]. To verify this view, XPS analysis has been used to measure the contents of copper with different valence in the fresh and the spent catalysts. The results are shown in Fig. 6 and Table-4.

Fig. 6a shows the XPS survey of the fresh and spent 0.8Cu-0.2Mn-Si and Cu-Si catalysts. It can be seen from the survey, the main elements in the fresh and the spent catalysts are Si, Cu, Mn and C. The presences of carbon in the survey verify the results of

the TG analysis of the spent catalysts, that is, the catalysts' thermal weight loss may be partly caused by the loss of the coke.

The values of the binding energy of Cu^{2+} in $Cu2p_{3/2}$ spectra are 934.17-944.31 eV while those in $Cu2p_{1/2}$ spectra are 954.37-962.53 eV. There is a difference value of about 20 eV between them. The values of the binding energy of Cu^{+} and Cu^{0} in $Cu2p_{3/2}$ spectra are 932.11-933.81 eV while those in $Cu2p_{1/2}$ spectra are 952.02-954.4 eV. From these data we can see that the binding energy of Cu^{2+} is slightly greater than that of Cu^{+} and Cu^{0}. The shake-up peaks of Cu^{2+} with a binding energy between 940-945 eV are very obvious in the fresh catalysts, while they almost disappear in the spent catalysts.

From Fig. 6b and Table-4, it can be seen that after adding manganese species, the contents of reducing copper (Cu^{+} and Cu^{0}) in the fresh catalysts are increased, which indicates that the copper-manganese complex oxides are formed as mentioned in the XRD results. It can be seen from Table-4, (Cu^{0}+ Cu^{+})/ Cu^{2+} in the spent 0.8Cu-0.2Mn-Si catalysts is 1.16 while that in the spent Cu-Si catalysts is 1.05. These Cu^{0} and Cu^{+} species are produced by the reduction of H_2 during the reaction. These results indicate that the addition of manganese in the Cu/SiO_2 catalysts plays an important role in the reduction process. The formation of copper-manganese complexes after the addition of manganese makes it easier to be reduced, which is the main reason for the improvement of the catalytic activity. These results obtained from XPS are consistent with those from XRD and H_2-TPR.

Influence of Cu/Mn mole ratios on catalytic performance

Fig. 7 and Fig. 8 show the experimental results of the catalysts with different molar ratios of Cu to Mn in the dehydrogenation reaction of 2-butanol at 240 ℃, H_2: N_2=5: 95. It can be seen from Fig. 7 that when the molar ratios of Cu to Mn gradually increase from 0: 1 to 0.8: 0.2, the conversion of 2-butanol increases from 18% to 94.9%. However, it is worth noting that when the molar ratios of Cu to Mn continue to increase, that is to say, if there is less Mn species in the catalysts, *i.e.* 0.9Cu-0.1Mn-Si and Cu-Si catalysts, the conversion of 2-butanol begins to decrease.

Being referred Fig. 1 and Fig. 7, it can be seen that the activity of catalysts highly depends on their components. Among them, the activity of Mn-Si catalysts is the lowest because there are only some reduced species of Mn_2O_3 in Mn-Si catalysts. In contrast, the activity of Cu-Si catalysts is very high although there are only some reduced species of CuO in Cu-Si catalysts. It indicates that the main active species in Cu-Mn-Si catalysts may be copper species, not manganese species.

Being referred Fig. 3 and Fig. 7, the comparisons of the reaction results of the catalysts containing both Cu and Mn were made. It can be seen that the activities of the Cu-Mn-Si catalysts are highly correlated with the reduction temperature in the H_2-TPR experiments. The catalyst of 0.8Cu-0.2Mn-Si has the best catalytic activity as it has the lowest reduction temperature. Comparison with the results of the TG analysis in Fig. 4, it can be seen that this result may relate to the ratio of the amounts of copper- manganese complex oxides and those of copper oxides in the catalysts.

It can be seen from Fig. 8 that the values of the selectivity of methyl ethyl ketone of almost all the catalysts (Cu-Si, Mn-Si and Cu-Mn-Si) are greater than 97%. The selectivity of methyl ethyl ketone can reach 98% when 0.8Cu-0.2Mn-Si catalysts are used.

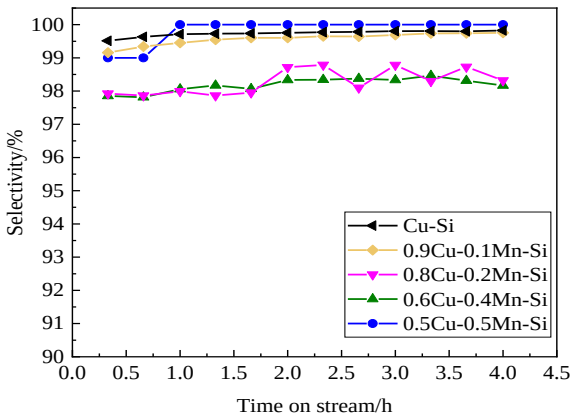

Fig. 8: Influence of Cu/Mn mole ratios on methyl ethyl ketone selectivity.

Fig. 9 shows that the TOF values increase gradually with the increase of Mn in the catalysts. This means that the utilization of Cu can be improved by doping manganese species. The addition of manganese produces copper manganese complex, which improves the dispersion of copper components and reduces its reduction temperature. The characteristics of being easy to be reduced of the copper manganese complex increase the contents of reducing active components in the catalyst, and promotes the improvement of the catalytic performance.

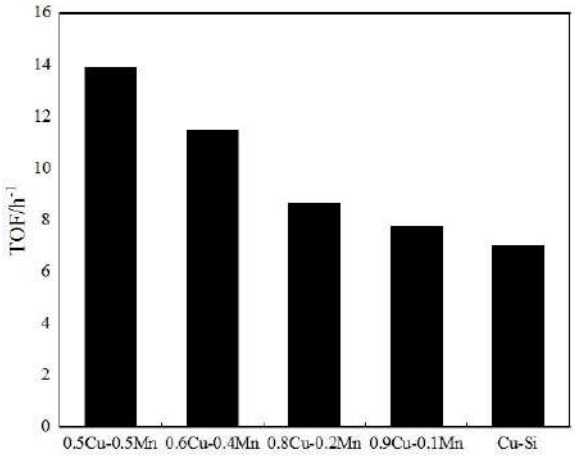

Fig. 9: TOF value of Cu/Mn mole ratios for the dehydrogenation reaction of 2-butanol.

Conclusion

The Cu-Mn-Si catalysts with different mole ratios of Cu to Mn were prepared by co-precipitation method. The performances of the catalysts for the dehydrogenation reaction of 2-butanol to methyl ethyl ketone were tested. Some conclusions have been made as follows.

1. The performances of Cu-Si catalysts for the dehydrogenation reaction of 2-butanol to methyl ethyl ketone can be significantly improved by the addition of Mn species. The conversion of 2-butanol can reach 94.9% and the selectivity of methyl ethyl ketone can reach 98% at the mole ratio of Cu: Mn: Si is 0.8: 0.2: 1.
2. The XRD characterizations show that, copper-manganese complex oxides are formed in the catalysts by the addition of Mn species. Among all Cu-Mn-Si catalysts, it has the highest crystallinity and the smallest size when the mole ratio of Cu: Mn: Si is 0.9: 0.1: 1; It has the best dispersion and the most uniform particle size when the mole ratio of Cu: Mn: Si is 0.5: 0.5: 1; It has the lowest reduction temperature when the mole ratio of Cu: Mn: Si is 0.8: 0.2: 1.
3. The performances of the catalysts are more determined by their reducibility. The specific surface area and the pore structures of the catalysts are not the most important factors to determine their catalytic performance.
4. The results obtained by the TG and the XPS analysis of the fresh and the spent catalysts show that there are more reduced species in the spent catalysts. The main active components of the catalysts are the copper species at lower valence, *i.e.*, Cu^0 and Cu^+. The addition of manganese species is helpful for the existence of the copper species at lower valence.

Acknowledgements

This work was supported by Shenyang Science and Technology Bureau (No. RC190323) and Liaoning Provincial Department of Education (Nos. LJKMZ20220764, LJ2019001, No. LQ2020004) and the Funds of Liaoning Provincial Department of Science and Technology (Nos. 2019-BS-192, 2023) and the Talents Funding Project of Liaoning Provincial Department of Human Resources and Social Security (No. 2020B085).

References

1. Z.H. Liu, W.Z. Huo and H. Ma, Development and commercial application of methyl-ethyl-ketone production technology, J. *Chin. J. Chem. Eng.*, **14**, 5 (2006).
2. E. Geravand, Z. Shariatinia and F. Yaripour, Synthesis of copper-silica nanosized catalysts for 2-butanol dehydrogenation and optimization of preparation parameters by response surface method , J. *Chem. Eng. Res. Des.*, **96**, 10 (2015).
3. A.J. Marchi, J.L.G. Fieero and J. Santamaria, Dehydrogenation of isopropanol alcohol on a Cu/SiO_2 catalyst: a study of the activity evolution and reactivation of the catalyst, J. *Apple. Catal. A.*, **142**, 10 (1996).
4. H.H. Yang, Y.Y. Chen and X.J. Cui, A highly stable copper-based catalyst for clarifying the catalytic roles of Cu^0 and Cu^+ species in methanol dehydrogenation, J. *Angew. Chem. Int. Ed.*, **57**, 7 (2018).
5. M.S. Li, Y.F. Hao and C.-L. Fernando, “Hydrogen-Free”hydrogenation of nitrobenzene over Cu/SiO_2 via coupling with 2-butanol dehydrogenation, J. *Top. Catal.*, **58**, 4 (2015).
6. B. Wang, M.M. Jin and H. An, Hydrogenation performance of acetophenone to 1-phenylethanol on high active nano Cu/SiO_2 catalyst, J. *Catal. Lett.*, **150**, 1 (2020).
7. D. J. Thomas, J. T. Wehrli and M. S. Wainwright, Hydrogenolysis of diethyl oxalate over copper-based catalysts, J. *Apple. Catal. A.*, **86**, 2 (1992).
8. J. Wu, Y.M. Shen and C.H. Liu, Vapor phase hydrogenation of furfural to alcohol over environmentally friendly $Cu-Ca/SiO_2$ catalyst, J. *Catal. Commu.*, **6**, 6 (2005).
9. W. Shen, C. Pan and X.Y. Yang, Coupling reaction of 1,4-butanediol with maleic anhydride over $Cr-Cu/SiO_2$ catalysts, J. *Acta Chim. Sin.*, **66**, 11 (2008).
10. Y.J. Tu and Y.W. Chen, Effects of alkaline-earth

oxide additives on silica-supported copper catalysts in ethanol dehydrogenation, J. *Ind. Eng. Chem. Res.*, **37**, 1 (1998).
11. V.C. Deborah, A.P. Carlos and M.M.S. Vera, Stability and selectivity of bimetallic Cu-Co/SiO_2 catalysts for cyclohexanol dehydrogenation, J. *Apple. Catal. A.*, **176**, 2 (1999).
12. D.H. Ji, W.C. Zhu and Z.L. Wang, Dehydrogenation of cyclohexanol on Cu-ZnO/SiO_2 catalysts: the role of copper species, J. *Catal. Commun.*, **8**, 12 (2007).
13. T. Feckensten, J. Pohl and F.J. Carduck, Process for the hydrogenation of fatty acid methyl esters in a pressure range of 20 to 100 bars, Patent-EP0300346B1 (1989).
14. S.B. Danny, E.K. Poels and A. Bliek, Ester hydrogenolysis over promoted Cu/SiO_2 catalysts, J. *Apple. Catal. A.*, **184**, 2 (1999).
15. G.C. Chinchen, K.C. Waugh and D.A. Whand, The activity and state of the copper surface in methanol synthesis catalysts, J. *Appl. Catal.*, **25**, 2 (1986).
16. Y. Zhang, C.L. Ye and C.L. Guo, In_2O_3-modified Cu/SiO_2 as an active and stable catalyst for the hydrogenation of methyl acetate to ethanol, J. *Chinese. J. Catal.*, **39**, 1 (2018).
17. P. Decky, A. B. Wieckowski and L. Najder-kozdrowska, EPR study of dealuminated HY zeolite and silica containing Cu-Mn-Zn spinels: the effect of support, J. *Acta Phys. Pol. A.*, **132**, 1 (2017).
18. J.H. Li, A.R. Mao and W. Yao, Iridium supported on porous polypyridine-oxadiazole as high-activity and recyclable catalyst for the borrowing hydrogen reaction, J. *Green Chem*., **24**, 2602(2022).
19. J.H. Li, M. Yu and Z.C. Duan, Porous cross-linked polymer copper and iridium catalyzed the synthesis of quinoxalines and functionalized ketones under solvent-free conditions, J. *Mater. Chem. Front.*, **42,** 190(2021).
20. G. Ali, J. Nisar and A. Shah, Thermo-catalytic decomposition of polystryrene waste: Comparative analysis using different kinetic models, J. *Waste Manage. Res.*, **38**, 2(2019).
21. J.H. Li, Y.K. Yang and W.K. Hu, Catalytic synthesis of pyrazine and ketone derivatives by unsymmetrical triazolyl-naphthyridinyl-pyridine copper, J. *Chin.J.Org.Chem.*, **42**, 190(2022).
22. J.H. Li, H.Q. Liu and H.Y. Zhu, Highly efficient and recyclable porous organic polymer supported iridium catalysts for dehydrogenation and borrowing hydrogen reactions in water, J. *ChemCatChem*., **5**, 7861(2021).
23. J.H. Li, H.Q. Liu and B. Zhang, Synthesis of supported indazolyl-pyridyl-quinoline iridium catalyst and its application to N-Alkylation of 2-aminobenzothiazoles, J. *Chin.J.Org.Chem.*, **42**, 619 (2022).